

Resonant nonradiative energy transfer in CdSe/ZnS core/shell nanocrystal solids enhances hybrid white light emitting diodes

Sedat Nizamoglu and Hilmi Volkan Demir

Department of Electrical and Electronics Engineering, Department of Physics,
Nanotechnology Research Center, and Institute of Materials Science and Nanotechnology,
Bilkent University, Ankara, Turkey TR-06800
volkan@bilkent.edu.tr

Abstract: We propose and demonstrate hybrid white light emitting diodes enhanced with resonant nonradiative energy transfer in CdSe/ZnS core/shell nanocrystal solids integrated on near-UV InGaN/GaN LEDs. We observe a relative quantum efficiency enhancement of 13.2 percent for the acceptor nanocrystals in the energy gradient mixed assembly, compared to the monodisperse phase. This enhancement is attributed to the ability to recycle trapped excitons into nanocrystals using nonradiative energy transfer. We present the time-resolved photoluminescence of these nanocrystal solids to reveal the kinetics of their energy transfer and their steady-state photoluminescence to exhibit the resulting quantum efficiency enhancement.

©2008 Optical Society of America

OCIS codes: (250.0250) Optoelectronics; (250.5230) Photoluminescence; (160.2540) Fluorescent and luminescent materials; Nanocrystals, quantum dots; Energy transfer.

References and links

1. S. Gaponenko, *Optical properties of semiconductor nanocrystals* (Cambridge University Press, 1998).
2. A. L. Rogach, A. Eychmüller, S. G. Hickey, and S. V. Kershaw, "Infrared emitting colloidal nanocrystals: synthesis, assembly, spectroscopy, and applications," *Small* **3**, 536 (2007).
3. V. Klimov, A. Mikhailovsky, S. Xu, A. Malko, J. Hollingsworth, C. Leatherdale, and M. Bawendi, "Optical gain and stimulated emission in nanocrystal quantum dots," *Science* **290**, 314–317 (2000).
4. J. H. Ahn, C. Bertoni, S. Dunn, C. Wang, D. V. Talapin, N. Gaponik, A. Eychmüller, Y. Hua, M. R. Bryce, and M. C. Petty, "White organic light emitting devices incorporating nanoparticles of II-VI semiconductors," *Nanotechnology* **18**, 335202 (2007).
5. E. Mutlugun, I. M. Soganci, and H. V. Demir, "Nanocrystal hybridized scintillators for enhanced detection and imaging on Si platforms in UV," *Opt. Express* **15**, 1128-1134 (2007).
6. I. Gur, N. A. Fromer, M. L. Geier, and A. P. Alivisatos, "Air-stable all inorganic nanocrystal solar cells processed from solution," *Science* **310**, 462-465 (2005).
7. O. Kulakovich, N. Strekal, A. Yaroshevich, S. Maskevich, S. Gaponenko, I. Nabiev, U. Woggon, and M. Artemyev, "Enhanced luminescence of CdSe quantum dots on gold colloids," *Nano Lett.* **2**, 1449-1452 (2002).
8. I. M. Soganci, S. Nizamoglu, E. Mutlugun, O. Akin, and H. V. Demir, "Localized plasmon-engineered spontaneous emission of CdSe/ZnS nanocrystals closely-packed in the proximity of Ag nanoisland films for controlling emission linewidth, peak, and intensity," *Opt. Express* **15**, 14289-14298 (2007).
9. S. Nizamoglu, G. Zengin, and H. V. Demir, "Color-converting combinations of nanocrystal emitters for warm-white light generation with high color rendering index," *Appl. Phys. Lett.* **92**, 031102 (2008).
10. H. Chen, D. Yeh, C. Lu, C. Huang, W. Shiao, J. Huang, C. C. Yang, I. Liu, and W. Su, "White Light Generation With CdSe–ZnS Nanocrystals Coated on an InGaN–GaN Quantum-Well Blue/Green Two-Wavelength Light-Emitting Diode," *IEEE Photon. Technol. Lett.* **18**, 1430-1432 (2006).
11. H. Chen, C. Hsu, and H. Hong, "InGaN–CdSe–ZnSe Quantum Dots White LEDs," *IEEE Photon. Technol. Lett.* **18**, 193-195 (2006).
12. H. V. Demir, S. Nizamoglu, T. Ozel, E. Mutlugun, I. O. Hoyal, E. Sari, E. Holder, and N. Tian, "White light generation tuned by dual hybridization of nanocrystals and conjugated polymers," *New J. Phys.* **9**, 362 (2007).

13. M. Ali, S. Chattopadhyay, A. Nag, A. Kumar, S. Sapra, S. Chakraborty, and D. D. Sarma, "White-light emission from a blend of CdSeS nanocrystals of different Se:S ratio," *Nanotechnology* **18**, 075401 (2007).
14. S. Nizamoglu and H. V. Demir, "Nanocrystal based hybrid white light generation with tunable color parameters," *J. Opt. A: Pure Appl. Opt.* **9**, S419-S424 (2007).
15. S. Nizamoglu and H. V. Demir, "Hybrid white light sources based on layer-by-layer assembly of nanocrystals on near-UV emitting diodes," *Nanotechnology* **18**, 405702 (2007).
16. A. A. Chistyakov, I. L. Martynov, K. E. Mochalov, V. A. Oleinikov, S. V. Sizova, E. A. Ustinovich, and K. V. Zakharchenko, "Interaction of CdSe/ZnS core-shell semiconductor nanocrystals in solid thin films," *Laser Phys.* **16**, 1625 (2006).
17. T. A. Klar, T. Franzl, A. L. Rogach, and J. Feldmann, "Super efficient exciton funneling in layer-by-layer semiconductor nanocrystal structures," *Adv. Mat.* **17**, 769 (2005).
18. C. R. Kagan, C. B. Murray, M. Nirmal, and M. G. Bawendi, "Electronic Energy Transfer in CdSe Quantum Dot Solids," *Phys. Rev. Lett.* **76**, 1517-1520 (1996).
19. C. R. Kagan, C. B. Murray, and M. G. Bawendi, "Long Range Resonance Transfer of Electronic Excitations in Close Packed CdSe Quantum Dot Solids," *Phys. Rev. B* **54**, 8633-8643 (1996).
20. S. A. Crooker, J. A. Hollingsworth, S. Tretiak, and V. I. Klimov, "Spectrally Resolved Dynamics of Energy Transfer in Quantum-Dot Assemblies: Toward Engineered Energy Flows in Artificial Materials," *Phys. Rev. Lett.* **89**, 186802 (2002).
21. M. Achermann, M. A. Petruska, S. A. Crooker, and V. I. Klimov, "Picosecond energy transfer in quantum dot Langmuir-Blodgett nanoassemblies," *J. Phys. Chem. B* **107**, 13782 (2003).
22. T. Franzl, D. S. Koktysh, T. A. Klar, A. L. Rogach, J. Feldmann, and N. Gaponik, "Fast energy transfer in layer-by-layer assembled CdTe nanocrystal bilayers," *Appl. Phys. Lett.* **84**, 2904 (2004).
23. T. Franzl, A. Shavel, A. L. Rogach, N. Gaponik, T. A. Klar, A. Eychemüller, and J. Feldmann, "High rate unidirectional energy transfer in directly assembled CdTe nanocrystal bilayers," *Small* **1**, 392 (2005).
24. T. Franzl, T. A. Klar, S. Schietinger, A. L. Rogach, and J. Feldmann, "Exciton recycling in graded gap nanocrystal structures," *Nano Lett.* **4**, 1599 (2004).
25. M. Achermann, M. A. Petruska, S. Kos, D. L. Smith, D. D. Koleske, and V. I. Klimov, "Energy-transfer pumping of semiconductor nanocrystals using an epitaxial quantum well," *Nature* **429**, 642 (2004).
26. J. Malicka, I. Gryczynski, J. Fang, J. Kusba, and J. R. Lakowicz, "Increased resonance energy transfer between fluorophores bound to DNA in proximity to metallic silver particles," *Anal. Biochem.* **315**, 160 (2003).
27. S. J. Rosenthal, "Bar-coding biomolecules with fluorescent nanocrystals," *Nat. Biotechnol.* **19**, 621 (2001).
28. J. Kimura, S. Maenosono, and Y. Yamaguchi, "Near-field optical recording on a CdSe nanocrystal thin film," *Nanotechnology* **14**, 69 (2003).
29. S. Maenosono, E. Ozaki, K. Yoshie, and Y. Yamaguchi, "Nonlinear photoluminescence behavior in closely packed CdSe nanocrystal thin films," *Jpn. J. Appl. Phys.* **40**, L. 638 (2001).
30. E. Sari, S. Nizamoglu, T. Ozel, and H. V. Demir, "Blue quantum electroabsorption modulators based on reversed quantum confined Stark effect with blue shift," *Appl. Phys. Lett.* **90**, 011101 (2007).
31. M. B. Yairi, H. V. Demir, and D. A. B. Miller, "Optically controlled optical gate with an optoelectronic dual diode structure: theory and experiment," *J. Opt. Quantum Electron.* **33**, 1035-1054 (2001).
32. H. V. Demir, V. A. Sabnis, O. Fidaner, J. S. Harris, Jr., D. A. B. Miller, and J.-F. Zheng, "Dual-diode quantum-well modulator for C-band wavelength conversion and broadcasting," *Opt. Express* **12**, 310-316 (2004).
33. T. Ozel, E. Sari, S. Nizamoglu, and H. V. Demir, "Violet to deep-ultraviolet InGaN/GaN and GaN/AlGaIn quantum structures for UV electroabsorption modulators," *J. Appl. Phys.* **102**, 113101 (2007).
34. S. Nizamoglu, T. Ozel, E. Sari, and H. V. Demir, "White light generation using CdSe/ZnS core-shell nanocrystals hybridized with InGaN/GaN light emitting diodes," *Nanotechnology* **18**, 065709 (2007).

Semiconductor nanocrystal (NC) quantum dots attract significant attention because of their size-tunable optical properties with large photoluminescence (PL) quantum yields and high photostability [1]. They also exhibit relatively narrow and symmetric PL with high photobleaching thresholds, and feature small spectral overlap between absorption and emission. Furthermore, for device applications, various common film deposition techniques (spin casting, dip coating, Langmuir-Blodgett, etc.) may be conveniently used to make uniform NC films in solid state. As a result, semiconductor NCs have been extensively exploited in a wide range of applications [1-15]. However, in those device applications, nanocrystals typically suffer from relatively low quantum efficiency when they are cast into solid form [16]. To address this problem, we investigate the use of Förster energy transfer in nanocrystal solids to increase their spontaneous emission rate in hybrid white light emitting diodes (WLEDs). The emission enhancement based on such carefully designed energy

transfer systems is critically important especially for white light emitting diodes in solid state lighting application, which is considered to make one of the next solid state frontiers.

The Förster energy transfer (ET) is the nonradiative transfer of excitation energy from an excited molecule (donor) to a ground-state molecule (acceptor) [17-25]. Kagan et al. first demonstrated ET in spin-cast films of closely packed CdSe core nanocrystals with different sizes [18,19]. Crooker et al. showed bilayer light-harvesting quantum dot films with an effective energy bandgap gradient structure with monolayer assemblies of CdSe/ZnS core/shell nanocrystals [20]. This energy gradient structure efficiently transported energy between nanocrystals in a submicron range much faster than their radiative decay rates [20,21]. Franzl et al. demonstrated energy transfer in bilayers of CdTe NCs by using oppositely charged polyelectrolyte linkers [22] and then without using any linker they revealed ET in bilayers of oppositely charged NCs [23]. They further showed a cascaded energy transfer having a funnel-like band gap profile structure by using distinctly sized CdTe nanocrystals [24]. Also, Klar et al. showed super efficient exciton funneling structure using layer-by-layer nanocrystals [17]. In that study it was demonstrated that using energy gradient structure not only excitons in radiative states are transferred, but also the trapped excitons that are generally nonradiatively recombined are recycled, resulting in an overall emission increase. Also, Achermann et al. demonstrated a none-white light emitting diode by pumping a single type of CdSe/ZnS nanocrystals using epitaxial quantum wells, i.e., excitation from quantum wells to nanocrystals [25]. However, the use of the Förster ET particularly in nanocrystal solids of white light emitting diodes has not been studied or demonstrated for solid state lighting to date.

In this work, for white light emitting diodes we propose and demonstrate the enhancement of spontaneous emission in integrated nanocrystal solids on hybrid WLED platforms. We use closely packed CdSe/ZnS core/shell nanocrystals of two carefully selected sizes with sufficient energy gradient (approximately 160 meV) hybridized on our near-UV InGaN/GaN LEDs for enhanced quantum efficiency of quantum dot solids. In such designed mixture of nanocrystal solids, the small quantum dots serve as donors and the large quantum dots as acceptors, leading to energy transfer from the small ones to the large ones. As a result, we observe an emission enhancement of 46% for the large dots residing in the mixed energy gradient assembly of small and large dots, with respect to the emission of only large dots. This corresponds to a 13.2% increase in the quantum efficiency of the large dots in the presence of the small dots, compared to the large dots alone. Here we investigate the Förster energy transfer using both steady-state and time-resolved spectroscopy of these nanocrystal solid samples. Their time-resolved photoluminescence, which reveals the kinetics of the energy transfer, and their spontaneous emission at the steady state, which exhibits the resulting quantum efficiency enhancement, together prove the action of energy transfer in nanocrystal solids.

To investigate Förster energy transfer, we use CdSe/ZnS core/shell nanocrystals from Evident Technologies with diameters of 7.7 nm and 8.2 nm emitting at 540 nm and 580 nm in solution, respectively. For control groups, we prepare two test solid films that consist of only small and only large quantum dots. For nonradiative Förster energy transfer, we prepare mixed assembly of both small and large nanocrystals by making their closely packed film. This solid film contains exactly the same total amount of large and small nanocrystals as in the control groups. For time-resolved spectroscopy measurements (shown in Fig. 1), we use a FluoTime 200 spectrometer (PicoQuant) with a time-correlated single photon counting (TCSPC) system of PicoHarp 300 with a calibrated time resolution of 4 ps. To pump nanocrystal solids, we use a laser head at an emission wavelength of 375 nm with light pulses as short as 70 ps and a photon multiplier tube (PMT) as the detector. Using an output monochromator, we characterize all of the prepared NC solids at 550 nm and 612 nm, corresponding to the peak emission wavelengths of the small NCs and the large NCs in the film, respectively. For the data analysis we use the software FluoFit to deconvolute the instrumental response. For steady-state spectroscopy measurements (shown in Fig. 2), we use

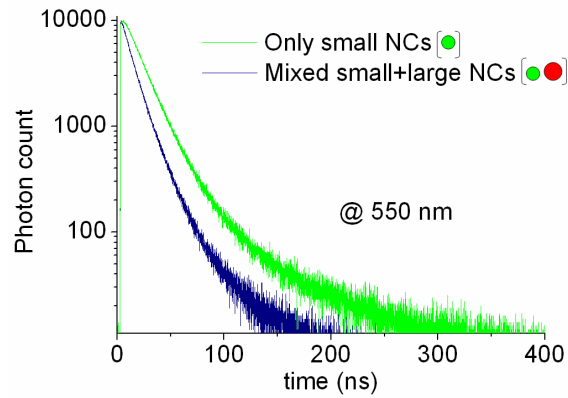
a Xenon halogen lamp in a monochromator as the excitation light source and an integrating sphere for collecting the total emission from the nanocrystal solids.

Figure 1(a) shows the time-resolved photoluminescence of only small nanocrystal solids along with that of mixed large and small solids, both at the emission wavelength of small dots (around 550 nm). Figure 1(b), on the other hand, depicts the time-resolved photoluminescence of only large nanocrystal solids along with that of mixed large and small solids, both at the emission wavelength of large dots (around 612 nm). In Fig. 1(a), the decay rate of the mixed nanocrystal solids at 550 nm is clearly observed to increase with respect to the only small dots because the small dots serving as donors in the mixture quench as a result of their excitation energy transferred to the acceptor large dots in the mixture. In contrast, in Fig. 1(b) the decay rate of the mixed nanocrystal solids at 612 nm is clearly observed to decrease with respect to the only large dots because the acceptor large dots take the transferred energy from the donor small dots. We fit our decay curves in Fig. 1(a) and (b) using a multiexponential model fit with convolution of the laser diode response at 375 nm; their fitting parameters are summarized in Table 1. Here the lifetime 1 (i.e., τ_1) is the general lifetime of the nanocrystals, which is on the order of tens of nanoseconds [16,25]. However, there exists another decay lifetime (i.e., τ_2), which is more than 40 ns. The amplitude of the long decay component is relatively weak when we compare its amplitude (with counts of hundreds) to that of the general nanocrystal decay time amplitude (with counts of thousands). We attribute these slow and weak decay components to environmental effects. Furthermore, for mixed small and large nanocrystal case at 612 nm, we have a third lifetime component (i.e., τ_3) of 2.84 ns. This third component is an additional decay for small dots as donors, but it also appears as an additional energy increase for large dots as acceptors in the mixed case (In Table 1, to differentiate the energy increase component, we put a minus sign in the amplitude). In addition, we also calculate the intensity averaged lifetime components (i.e., τ_{avg}) using equation (1) (where A_i and τ_i refer to amplitudes and lifetimes, respectively) to observe the quenching for small dots and the energy feeding in large dots. The intensity weighted average decay time constant for the small dots at 550 nm is found to decrease from 15.53 ns to 10.58 ns as a consequence of quenching when the small dots are placed in the close vicinity of the large dots in the mixed assembly. On the other hand, the intensity weighted average decay time constant of large dots in the mixed assembly at 612 nm is found to increase from 17.66 ns to 22.59 ns with respect to only large dots as a result of the energy transfer. Also, using equation (2), we calculate the amplitude weighted average lifetime (i.e., τ_{amp_avg}) of only small nanocrystals and mixed small-large nanocrystals case at 550 nm. Furthermore, we determine the efficiency of energy transfer using equation (3) where $\tau_{amp_avg_DA}$ refers to the amplitude weighted average lifetime of mixed small (Donor) and large (Acceptor) nanocrystals and $\tau_{amp_avg_D}$ refers to the amplitude weighted average lifetime of only small (Donor) nanocrystals [26]. As a result, the efficiency of energy transfer in the mixed small and large nanocrystals reaches a relatively high level of 55.58%.

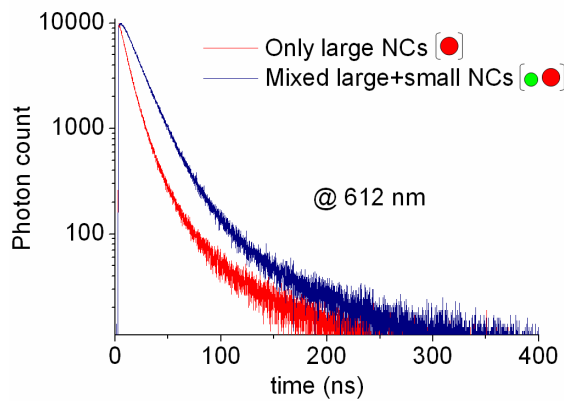
$$\tau_{avg} = \frac{\sum_i A_i \tau_i^2}{\sum_i A_i \tau_i} \quad (1)$$

$$\tau_{amp_avg} = \frac{\sum_i A_i \tau_i}{\sum_i A_i} \quad (2)$$

$$E = 1 - \frac{\tau_{amp_avg_DA}}{\tau_{amp_avg_D}} \quad (3)$$



(a)



(b)

Fig. 1. Time-resolved photoluminescence of (a) only small nanocrystal solids (with a diameter of 7.7 nm) and mixed nanocrystal solids (with diameters of 8.2 and 7.7 nm) for emission at 550 nm, and (b) only large nanocrystal solids (with a diameter of 8.2 nm) and mixed nanocrystal solids (with diameters of 8.2 and 7.7 nm) for emission at 612 nm.

Table 1. The fitting parameters of time-resolved spectra in Fig. 1(a)-(b). A_n and τ_n are the amplitudes and decay time constants, for $n=1, 2, 3$; τ_{avg} and $\tau_{\text{amp-avg}}$ are the intensity and amplitude weighted average decay time constants.

	Only small nanocrystals (at 550 nm)	Mixed small and large nanocrystals (at 550 nm)	Only large nanocrystals (at 612 nm)	Mixed small and large nanocrystals (at 612 nm)
A_1 [Counts]	10313.6	4189.2	10171	12588
τ_1 [ns]	12.06	10.00	9.936	16.96
A_2 [Counts]	410.3	110.9	499.9	416.0
τ_2 [ns]	41.133	46.33	42.597	61.90
A_3 [Counts]	-	7248	-	-3298
τ_3 [ns]	-	2.84	-	2.84
τ_{avg} [ns]	15.53	10.58	15.62	22.57
$\tau_{\text{amp-avg}}$ [ns]	13.17	5.85	-	-

We also present the steady-state spectroscopy measurements of these nanocrystal solid samples that are taken using an integrating sphere to observe the effect of this Förster energy transfer on the spontaneous emission spectra and the associated quantum efficiencies. In Fig.

2, the photoluminescence and absorption spectra of only large, only small, and mixed large and small nanocrystal assemblies are shown. In the mixed large and small nanocrystal solids, the peak at 550 nm decreases with respect to only small nanocrystal solids due to transferring its excitation energy to the large nanocrystals (i.e., quenching of the small nanocrystals) and, for the same reason, the peak at 612 nm increases as a result of the transferred energy. Although the number of large dots in mixed assembly is the same as only large dots, we observe a 46% enhancement in the emission of large dots in the mixed assembly compared to only large solids. Furthermore, to investigate the quantum efficiencies (QEs) of these solid samples, we experimentally measure QE of the mixed solids to be 29.1% in the integrating sphere. It is known that the emission spectrum of nanocrystals exhibits a Gaussian like emission line shape on a wavelength scale. This kind of Gaussian fit is also used in several references [27-29]. Using Gaussian fits to the steady-state luminescence of the mixed nanocrystal solids and weighting only according to the emission levels of small and large dots alone, without considering energy transfer, we calculate the expected QE of the mixed solids to be only 25.7%. Therefore, we find out that the experimentally measured QE is 13.2 percent better than the predicted one because of the energy transfer. It is well known that excitons are more likely to be captured in surface traps leading to non-radiative recombination in defect-rich NCs, while defect-poor NCs exhibit a higher probability for radiative recombination. Using energy transfer, it is possible to transfer the excitation energy of trapped excitons from defect-rich NCs in film to proximal defect-poor NCs, as extensively discussed in [17]. Therefore, the difference in the measured and predicted efficiencies is attributed to the portion of trapped excitons recycled by the energy transfer to additionally contribute to the emission. Furthermore, we also observe that the orange emission of large nanocrystals in the mixed assembly is red shifted with respect to the case of only large nanocrystals. This red shift is a typical result of the dipole-dipole interaction. Among the orange emitting nanocrystals (acceptors), those with slightly larger size (in their size distribution of <5%) accepts more energy from green emitting nanocrystals (donors), leading to a further red shift. A similar situation occurs also in single-sized nanocrystals in film with a red shifted and modified emission line shape due to inhomogeneous size distribution as in [19].

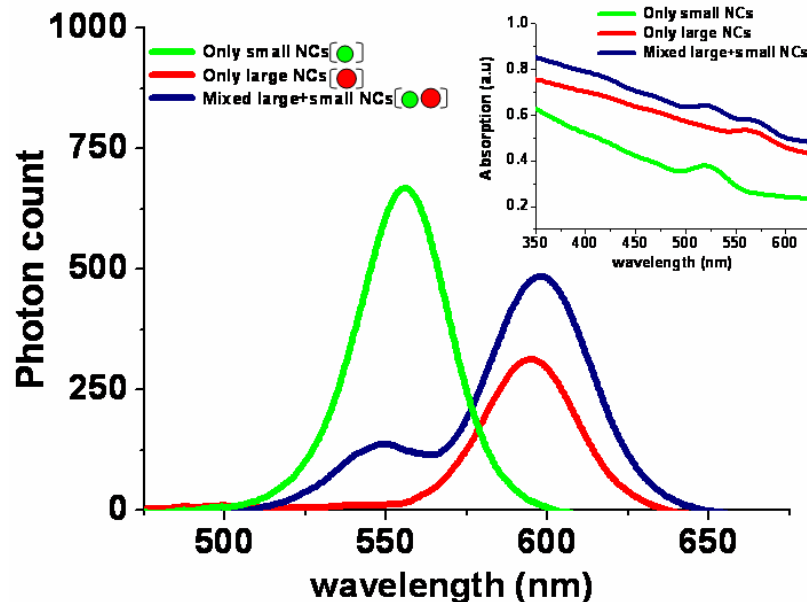


Fig. 2. Photoluminescence spectra of only large nanocrystals (8.2 nm), only small nanocrystals (7.7 nm) and mixed large-small nanocrystals (8.2 and 7.7 nm, respectively) along with their absorption spectra shown in the inset.

We employ these mixed large-small nanocrystal assemblies that exhibit Förster energy transfer in white light generation. We use the same amount of nanocrystals in the mixed assembly on an InGaN/GaN n-UV LED emitting at 383 nm. Similar device fabrication and characterization methods are given in our previous works [30-34], and their design and growth procedures are described elsewhere [34]. The operating principle of this white light emitting diode relies on the hybrid use of the LED as the excitation source and the integrated nanocrystal solid film as the photoluminescent layer. Near-UV LED pumps all the integrated nanocrystal solids that in turn luminescence at their corresponding emission wavelengths, while the excitons in the small nanocrystals and the trapped excitons also further transfer their energy to the large nanocrystals. Consequently, the photoluminescence of these nanocrystals enhanced with the energy transfer and the electroluminescence of the LED contribute altogether to generate white light. In Fig. 3, the emission spectra of the hybrid device driven at various current injection levels at room temperature are shown. Here it is important to carefully balance the levels of green emission ($\lambda_{PL}=550$ nm) and orange emission ($\lambda_{PL}=592$ nm) from these nanocrystals to allow the near-UV tail of the LED emission to shift the tristimulus coordinates to the white region. The emission spectrum of hybrid LED corresponds to (x,y) tristimulus coordinates of (0.44,0.40) and a correlated color temperature of 2872 K. This very warm white light emitting diode with such a low correlated color temperature is particularly important for indoor illumination applications [9].

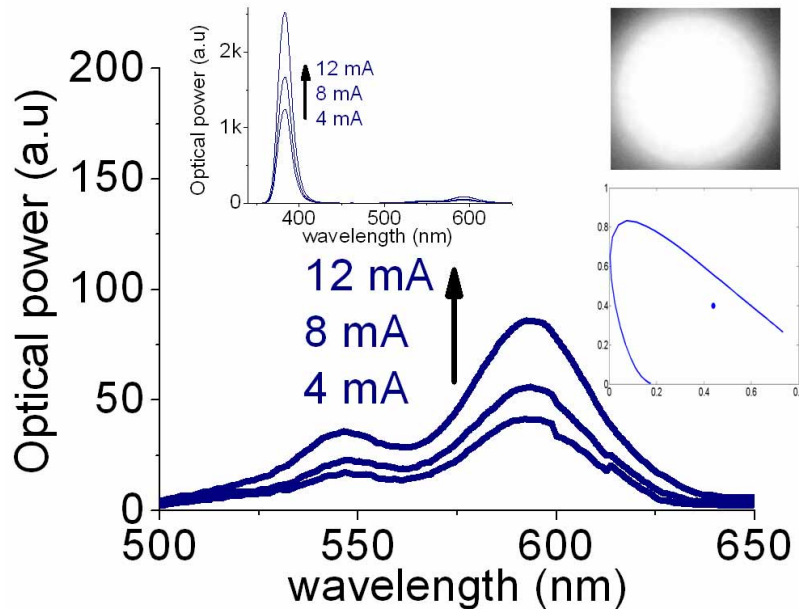


Fig. 3. Emission spectra of mixed CdSe/ZnS core/shell nanocrystals (with diameters of 8.2 nm and 7.7. nm) hybridized on n-UV InGaN/GaN light emitting diode driven at different levels of current injection at room temperature, along with the corresponding (x, y) coordinates and pictures of the hybrid WLED, while generating white light.

In conclusion, we demonstrated hybrid white light emitting diodes enhanced with resonant nonradiative energy transfer in CdSe/ZnS core/shell nanocrystal solids integrated on near-UV InGaN/GaN light emitting diodes. We observed a relative quantum efficiency enhancement of 13.2 percent for the acceptor nanocrystals in the energy gradient assembly by comparing with the monodisperse phase. We investigated the Förster energy transfer and quantum efficiency enhancement using both steady-state and time-resolved spectroscopy measurements. We believe that the resonant nonradiative energy transfer offers great potential to improve the efficiency of nanocrystal solids in lighting applications.

Acknowledgments

We are pleased to acknowledge PicoQuant GmbH Inc. for time-resolved spectroscopy (TRS) and Dr. Peter Kaspusta in particular for his kind assistance in TRS. This work is supported by EU-PHOREMOST NoE 511616 and EU-MC-IRG MOON 021391, and TUBITAK under the Project No. 106E020, 104E114, 107E088, 107E297, 105E065, and 105E066. Also, HVD acknowledges additional support from European Science Foundation European Young Investigator Award (ESF-EURYI) and Turkish Academy of Sciences Distinguished Young Scientist Award (TUBA-GEBIP) Programs.